



ELSEVIER

25 February 2002

PHYSICS LETTERS A

Physics Letters A 294 (2002) 210–216

www.elsevier.com/locate/pla

Convective wave front locking for a reaction–diffusion system in a conical flow reactor

P.V. Kuptsov^{a,*}, S.P. Kuznetsov^a, C. Knudsen^b

^a Institute of Radio Engineering and Electronics, Russian Academy of Science, Zelenaya 38, Saratov 410019, Russia

^b Department of Physics, The Technical University of Denmark, 2800 Kgs. Lyngby, Denmark

Received 5 June 2001; received in revised form 21 January 2002; accepted 23 January 2002

Communicated by A.P. Fordy

Abstract

We consider reaction–diffusion instabilities in a flow reactor whose cross-section slowly expands with increasing longitudinal coordinate (cone shaped reactor). Due to deceleration of the flow in this reactor, the instability is convective near the inlet to the reactor and absolute at the downstream end. In sustained regimes the two regions are separated by a stationary front. Results of numerical studies of the Brusselator flow model demonstrate that the front locking occurs at the place, where the flow velocity approximately corresponds to that of the transition from convective to absolute instability in a spatially uniform system. © 2002 Published by Elsevier Science B.V.

PACS: 82.40.Bj; 47.20.Ky

Keywords: Conical reactor; Wave front locking; Absolute and convective instabilities; Open flows; Reaction–diffusion systems; Hopf and Turing bifurcations

It is well known that instabilities in spatially uniform extended systems may be either convective or absolute [1–3]. In the first case, any initially localized perturbation, although growing, is advected with the flow in such way that observation at any fixed spatial point displays a decay of the perturbation to zero (Fig. 1(a)). In the second case, observation at a fixed point shows a growing perturbation that gradually occupies the whole spatial domain (Fig. 1(b)).

A particular class of media demonstrating the transition from convective to absolute instability is represented by reaction–diffusion systems with flow (Fig. 2(a)). If the flow rate is sufficiently high, the instability is of convective type, whereas for low flow rates the instability becomes absolute. The transition from convective to absolute instability occurs at some critical flow rate c_{ca} [4,5].

Let us consider a system with a flow velocity that slowly decreases along the spatial coordinate. For a fluid system such a condition may be realized by placing the flow inside a cone-shaped tube whose diameter slowly expands with the longitudinal coordinate (Fig. 2(b)). We may choose parameters in such a way

* Corresponding author.

E-mail addresses: kupav@mail.ru (P.V. Kuptsov), carsten.knudsen@fysik.dtu.dk (C. Knudsen).

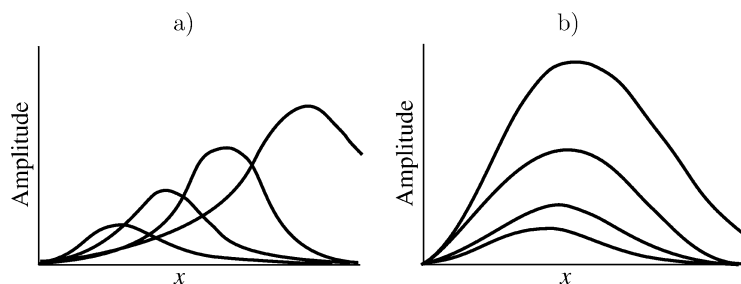


Fig. 1. Evolution of a localized perturbation in the uniform flow system: (a) convective instability, (b) absolute instability.

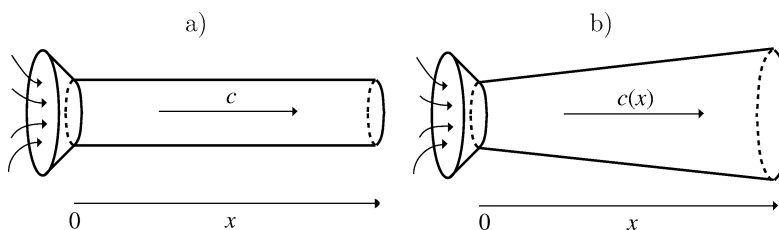


Fig. 2. Geometry of the reactor in the case of uniform flow (a) and for the cone system (b).

that the velocity near the inlet to the reactor corresponds to convective instability of a uniform flow, while at the downstream end it corresponds to absolute instability.

The transition from convective to absolute instability in the uniform flow system is associated with a change of direction of propagation for a front, that separates active and passive regions of the medium (see, e.g., [4,5]). In our nonuniform system, the front drifts along the flow being located in the domain of larger flow velocity (near the inlet), and in the opposite direction in the domain of slow velocity (near the downstream end). The stable position of the front is in the vicinity of the point x_{ca} where the flow velocity attains the critical value c_{ca} , that is, where the transition between convective and absolute instability occurs in the uniform system.

As suggested, the configuration of the reactor may easily be realized in practice, and it may provide a useful tool for experimental studies of details of the transition from convective to absolute instability. Indeed, by performing measurements on the amplitude distribution along the reactor, one can find the front position and, hence, estimate the critical velocity of the convective–absolute instability transition.

Let us now proceed by considering a concrete example, namely the well-known Brusselator flow sys-

tem, for which we will present numerical results supporting the outlined picture. The Brusselator is one of the canonical models of reaction–diffusion systems [6]. In a one-dimensional flow of constant rate the basic set of equations reads [5]

$$\begin{aligned} \frac{\partial U}{\partial t} + c \frac{\partial U}{\partial x} &= A - (B + 1)U + U^2V + \sigma \frac{\partial^2 U}{\partial x^2}, \\ \frac{\partial V}{\partial t} + c \frac{\partial V}{\partial x} &= BU - U^2V + \frac{\partial^2 V}{\partial x^2}. \end{aligned} \quad (1)$$

Here U and V denote dimensionless concentrations of the interacting chemical species, A and B are externally controlled feed concentrations, $c > 0$ is the velocity of flow, and $\sigma > 0$ is the ratio of the diffusion constants for the components U and V . The reagents are assumed to be pumped continuously into the reaction space from the left, see Fig. 2(a). System (1) has a homogeneous steady state

$$U_0 = A, \quad V_0 = B/A. \quad (2)$$

We suppose that the inlet concentrations correspond to the homogeneous state,

$$U|_{x=0} = U_0, \quad V|_{x=0} = V_0, \quad (3)$$

and that the right boundary condition at $x = L$ is free:

$$\left. \frac{\partial U}{\partial x} \right|_{x=L} = 0, \quad \left. \frac{\partial V}{\partial x} \right|_{x=L} = 0. \quad (4)$$

As the control parameters are varied one can observe a loss of stability for the spatially homogeneous state via a Hopf or via a Turing bifurcation [7]. The Hopf instability is associated with the appearance of spatially homogeneous oscillations. At fixed parameter values A , σ , and c , the bifurcation value of B for instability of this type is

$$B_H = 1 + A^2. \quad (5)$$

The Turing instability [8] manifests itself by the forming of a spatial structure with some fixed characteristic wavelength. This kind of instability can only appear when component V diffuses faster than U , i.e., at $\sigma < 1$. If this condition for the diffusion rates is satisfied, then the bifurcation value of B for the Turing instability is

$$B_T = (1 + A\sqrt{\sigma})^2. \quad (6)$$

Absolute and convective instabilities of Hopf and Turing type in system (1) were studied in [5] via so-called “pinch-point analysis”. The critical velocity c_{ca} may be found from the equations linearized near the homogeneous state for the variations $u = U - U_0$ and $v = V - V_0$. By means of exponential substitution $u, v \propto \exp(st + qx)$ the problem is reduced to the analysis of some functions of complex variables s and q (see [1–3,5] for details). The complex frequency s and wave number q obey the dispersion equation

$$(s + cq - B + 1 - \sigma q^2)(s + cq + A^2 - q^2) + AB^2 = 0. \quad (7)$$

Let us designate the left-hand side by $D(s, q)$, with $s = s(q)$ being the root of this quadratic equation. Then, as shown in [5], the critical velocity together with the complex unknowns s and q must satisfy the set of equations

$$D(s, q) = 0, \quad \text{Re}(\partial s(q)/\partial q) = 0. \quad (8)$$

Actually, besides the true solutions, these equations have some irrelevant spurious roots. To distinguish those corresponding to the actual convective–absolute transition one should either check the character of spatio-temporal evolution in numerical experiments in a vicinity of the found points, or perform some special analysis of the analytical properties of the complex roots of the dispersion equation $D(s, q) = 0$ [2,3,5].

When the instability is convective and the input concentrations differ from the homogeneous values, flow distributed oscillations appear that are spatially undamped for sufficiently large flow rate. These oscillations arise even if the Turing condition for the diffusion rates is not fulfilled and, actually, represent a new scenario for pattern formation in spatially distributed systems [5,9,10]. This effect must be taken into account in the experimental observations of the absolute and convective instabilities, because it can overshadow the convective instability.

Now let us turn to the flow system in the cone shaped reactor (Fig. 2(b)). To derive the respective dynamical equations let us first transform Eqs. (1) to three-dimensional form by means of the substitution

$$c \frac{\partial}{\partial x} \rightarrow \vec{c} \nabla, \quad \frac{\partial^2}{\partial x^2} \rightarrow \nabla^2, \quad (9)$$

where \vec{c} is the vector of the velocity. It is natural for the conical geometry of the reactor (see Fig. 2(b)) to rewrite the resulting equations in (nonstandard) spherical coordinates

$$x = r \cos \theta, \quad y = r \sin \theta \cos \phi, \\ z = r \sin \theta \sin \phi,$$

where the r -axis coincides with the axis of the cone and its origin lies in the intersection point of the cone wall continuation. To reduce the analysis to a one-dimensional problem we assume that U and V depend only on r and the velocity vector \vec{c} is co-directed with r -axis. To find the flow velocity as a function of r one can subdivide the reactor into a set of thin spherical layers of equal volume. The mixture of reagents is regarded as an uncompressed fluid, so passage of each layer must take equal time, and the velocity must comply with

$$c(x) = c_0 / (1 + \varphi x)^2. \quad (10)$$

Here c_0 is the inlet velocity, $\varphi = 1/r_0$ characterizes the angle of the cone, r_0 is the coordinate of the inlet, $x = r - r_0$. The final equations then take the following form:

$$\frac{\partial U}{\partial t} + \left(\frac{c_0}{(1 + \varphi x)^2} - \frac{2\sigma\varphi}{1 + \varphi x} \right) \frac{\partial U}{\partial x} \\ = A - (B + 1)U + U^2V + \sigma \frac{\partial^2 U}{\partial x^2},$$

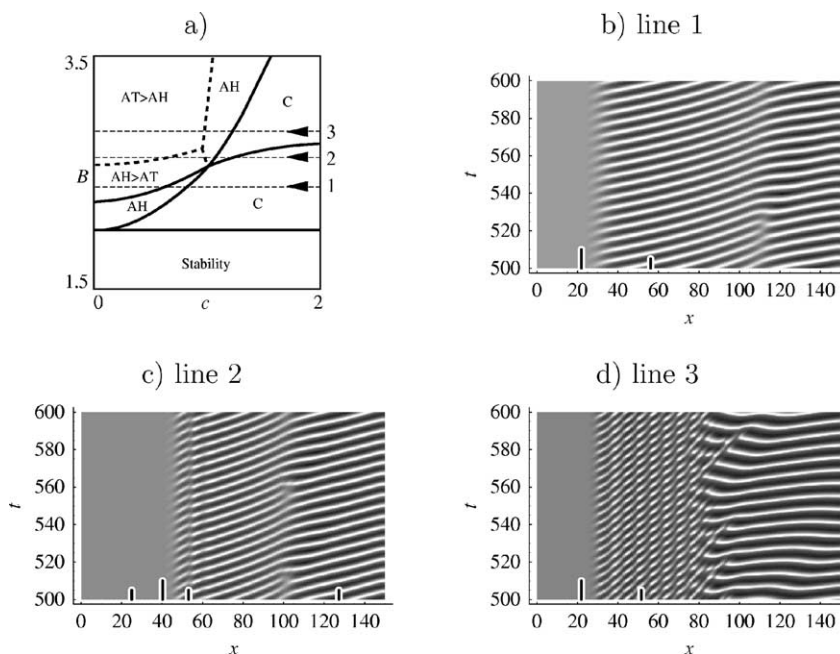


Fig. 3. Parameter plane of the uniform Brusselator flow system (1) (from [5]) (a) and spatio-temporal diagrams for the cone system, $A = 1$, $\sigma = 0.25$, $\varphi = 0.01$ (b)–(d). The horizontal lines on the parameter plane correspond to the values of B , at which the diagrams (b)–(d) are drawn; the regions of distinct behavior are marked by letters (H and T denote the Hopf and Turing instability, A and C designate the absolute and convective instability, symbol $>$ shows what instability has larger linear increment). On the spatio-temporal diagrams (b)–(d) the gray scales code the magnitude of U . Small vertical segments mark the places of intersection of the horizontal lines with the domain boundaries on the parameter plane diagram (a). The highest mark corresponds to the convective–absolute transition, i.e., the critical point x_{ca} . The parameter values are $B = 2.38$, $c_0 = 1$ (b), $B = 2.63$, $c_0 = 1.5$ (c), $B = 2.85$, $c_0 = 1.5$ (d).

$$\frac{\partial V}{\partial t} + \left(\frac{c_0}{(1 + \varphi x)^2} - \frac{2\varphi}{1 + \varphi x} \right) \frac{\partial V}{\partial x} = BU - U^2V + \frac{\partial^2 V}{\partial x^2}. \tag{11}$$

In the limit $\varphi \rightarrow 0$ we obviously return to the uniform system (1).

To solve the set of partial differential equations (1) and (11) we used an implicit finite-difference method of second order [11]. Typical values of the space and time discretization are around 0.1. Figs. 3 and 4 present diagrams illustrating spatio-temporal evolution of patterns in the flow system in the cone reactor with $\varphi = 0.01$ for some particular values of A and σ (see the figure captions). The first set of diagrams corresponds to the situation with the Hopf instability, and the second to the Turing instability. The spatio-temporal diagrams give evidence to the phenomenon of the wave front locking. Observe that no waves are present near the reactor inlet. The oscillations occur

to the right of some definite place, and the spatial location of the transition depends on parameters of the system.

In Figs. 3(a) and 4(a) we reproduce the charts of the parameter plane (c , B) found in [5] for the uniform system. In the cone system (11), the flow velocity varies from one cross-section of the reactor to another. This means that each of the spatio-temporal diagrams can be associated with some horizontal line on the parameter plane of Figs. 3(a) and 4(a).

As expected, the place of the front locking must correspond to the point, where the local velocity of the flow is equal to the critical value of the convective–absolute instability transition in the uniform system.

On the spatio-temporal diagrams small vertical segments are shown that mark points where the local flow velocity corresponds to the intersection of the horizontal lines with the bifurcation borders in the parameter plane. The largest mark designates the threshold of the absolute–convective instability transition point.

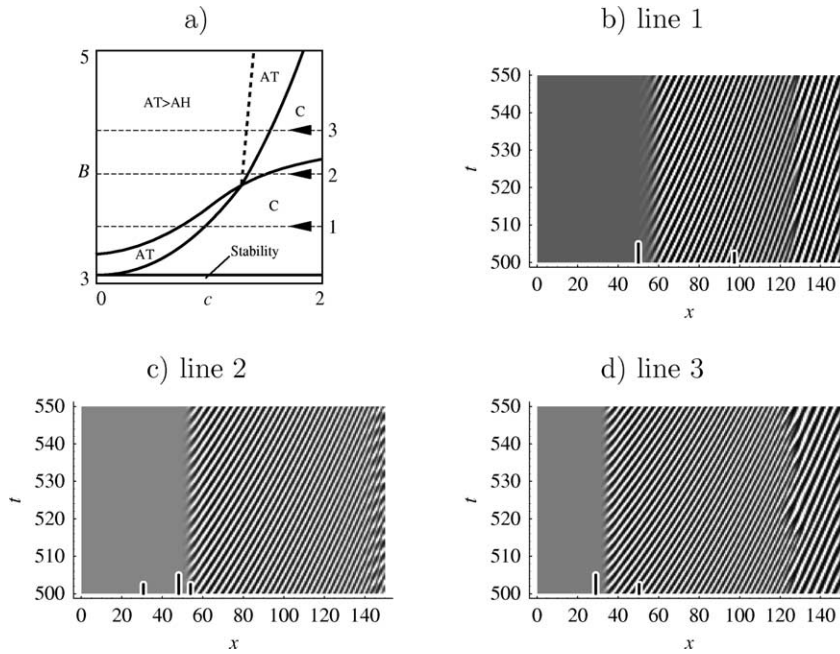


Fig. 4. Diagrams analogous to Fig. 3, but for $A = 1.5$. The remaining parameters are as follows: $B = 3.5$, $c_0 = 1.5$ (b), $B = 3.94$, $c_0 = 2$ (c), $B = 4.32$, $c_0 = 2$ (d).

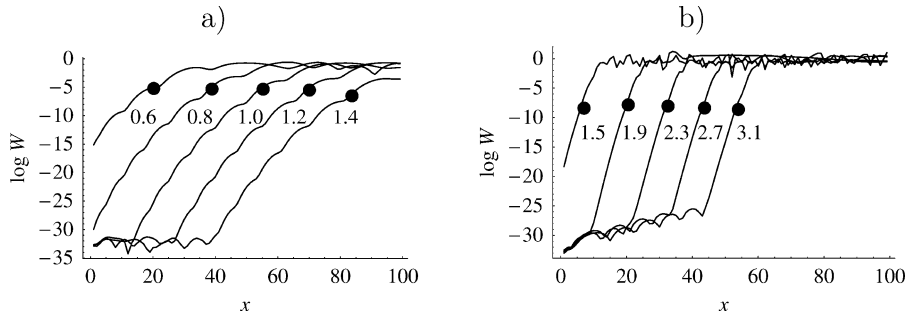


Fig. 5. Distribution of amplitude (12) over the reactor length after decay of transients at different inlet rates c_0 . Values of c_0 are indicated at the corresponding curves. The solid points on the curves represent the position of the critical points as found from the equation $c(x_{ca}) = c_{ca}$, accounting for (8) and (10). For both figures $A = 1$, $\sigma = 0.25$, and $\varphi = 0.01$. The remaining parameters are $B = 2.1$, $c_{ca} = 0.415$ (a) and $B = 3$, $c_{ca} = 1.308$ (b).

Observe that it is indeed close to the place of front locking.

Let us discuss in more detail the location of the place of the wave front locking and of the point of the critical velocity of the absolute–convective transition.

In Fig. 5 we present the distributions of the amplitudes of oscillations defined as

$$W = \sqrt{(U - U_0)^2 + (V - V_0)^2} \tag{12}$$

over the reactor length after decay of transients. Different curves correspond to different inlet rates c_0 . In fact, the front does not have well-defined boundaries, but we can attribute some characteristic width to it. Arbitrarily, we define the WFL region (WFL stands for wave front locking) as located between the points of amplitudes

$$W = e^{-20} \quad \text{and} \quad W = e^{-3}. \tag{13}$$

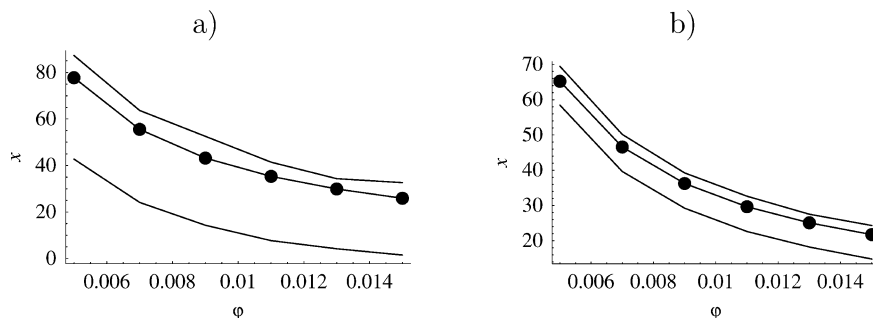


Fig. 6. Location of the borders of the WFL region (as defined by (13)) and the critical point versus the cone angle φ . For both figures $A = 1$, $\sigma = 0.25$. The rest parameters: $B = 2.1$, $c_0 = 0.8$ (a) and $B = 3$, $c_0 = 2.3$ (b).

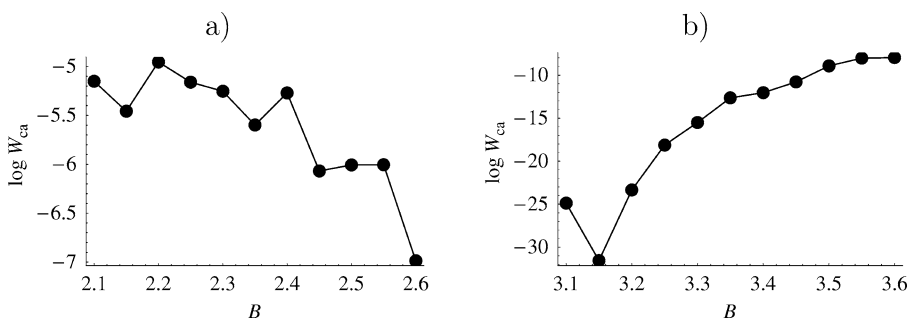


Fig. 7. Amplitude W observed at the critical point versus B . For both figures $\sigma = 0.25$, $\varphi = 0.01$. Panel (a) corresponds to the case of Hopf bifurcation, $A = 1$, $c_0 = 1.2$, and panel (b) to the case of Turing bifurcation, $A = 1.5$, $c_0 = 1.5$.

From Fig. 5 one can see that in dependence on the flow rate c_0 the distributions are simply shifted in space, but retain their shape. Fig. 6 shows the location of the WFL region and of the critical point versus the cone angle φ . Observe that the critical point retains its relative location inside the WFL region as the angle φ is changed. We observe that this is true at least in the range of velocities not too far from the critical value and at sufficiently small cone angles.

We conclude that from the location of the WFL region in the cone reactor one can extract information about the position of the critical point and, hence, about the critical velocity associated with the absolute–convective instability transition in the corresponding uniform flow system.

From Figs. 5 and 6 one can see that the location of the critical point in the WFL region depends on the parameter B . This dependence is illustrated in Fig. 7. Panel (a) corresponds to a region near the Hopf bifurcation and panel (b) to the Turing bifurcation. Note the apparent difference between the curves.

One more interesting feature of the conic flow system consists of the presence of “jumps” in the spatial distribution of the oscillation frequencies. As observed on the diagrams of Figs. 3 and 4, the active region of the medium consists of a number of domains separated by relatively narrow “domain walls”; each domain corresponds to approximately constant time period of oscillation. This may be explained as a competition between two factors. One factor is a change of the most favorable frequency of local oscillations down the flow, and the other is an interaction of the oscillations in spatially close regions, which tends to synchronize them. In fact, this is a phenomenon known as cluster synchronization which has been observed earlier in the numerical experiments with arrays of locally coupled self-oscillators [12]. We will present further details of a study of this phenomenon in the reaction–diffusion flow model elsewhere [13].

The problem of correspondence between the transition in a homogeneous system and patterns in a system with the control parameter changing in space is com-

plicated in the general case. The idea that those structure will develop which are stable in the corresponding system at the local values of the control parameter is not always correct [14]. In particular, it may not be the case for systems with subcritical transition [15]. In this Letter we discussed some features of spatio-temporal dynamics of a model of the reaction–diffusion flow system in a conical reactor with cross-section slowly expanding along the longitudinal coordinate. Due to the deceleration of the flow, the instability which is locally convective near the inlet becomes absolute near the opposite end of the reactor. We argued that there exist a correspondence between this system and the respective system with a constant flow. The observation of the front locking reveals the border between the convective and absolute instability, and this circumstance may be used in experimental studies.

Acknowledgements

We would like to thank E. Mosekilde for valuable discussions related to this work. P.V.K. acknowledges support from CRDF (grant REC-006). S.P.K. acknowledges support from RFBR (grant 00-02-17509).

References

- [1] L.D. Landau, E.M. Lifshitz, *Fluid Mechanics*, Pergamon, Oxford, 1959.
- [2] R.J. Briggs, *Electron Stream Interaction with Plasma*, MIT, Cambridge, 1964.
- [3] A. Bers, in: A.A. Galaev, R.N. Sudan (Eds.), *Handbook of Plasma Physics*, North-Holland, Amsterdam, 1983, p. 451.
- [4] A. Couairon, J.M. Chomaz, *Physica D* 108 (1997) 236.
- [5] S.P. Kuznetsov, E. Mosekilde, G. Dewel, P. Borckmans, *J. Chem. Phys.* 106 (1997) 7609.
- [6] I. Prigogine, R. Lefever, *J. Chem. Phys.* 48 (1968) 1965.
- [7] G. Nicolis, I. Prigogine, *Self-Organization in Nonequilibrium Systems*, Wiley, New York, 1977.
- [8] A.M. Turing, *Philos. Trans. R. Soc. B* 237 (1952) 37.
- [9] P. Andresén, M. Bache, G. Dewel, P. Borckmans, E. Mosekilde, *Phys. Rev. E* 60 (1999) 297.
- [10] M. Kærn, M. Menzinger, *Phys. Rev. E* 60 (1999) R3471.
- [11] W.H. Press, S.A. Teukolsky, W.T. Vetterling, B.P. Flannery, *Numerical Recipes in C*, Cambridge University Press, 1992.
- [12] G.V. Osipov, M.M. Sushchik, *Phys. Rev. E* 58 (1998) 7198.
- [13] P.V. Kuptsov, S.P. Kuznetsov, C. Knudsen, to appear.
- [14] P. Borckmans, A. De Wit, G. Dewel, *Physica A* 188 (1992) 137.
- [15] O. Jensen, E. Mosekilde, P. Borckmans, G. Dewel, *Phys. Scr.* 53 (1996) 243.